

UC Merced

UC Merced Previously Published Works

Title

Canopy effects on snow accumulation: Observations from lidar, canonical-view photos, and continuous ground measurements from sensor networks

Permalink

<https://escholarship.org/uc/item/35m8122d>

Journal

Remote Sensing, 10(11)

ISSN

2072-4292

Authors

Zheng, Z
Ma, Q
Qian, K
et al.

Publication Date

2018-11-01

DOI

10.3390/rs10111769

Peer reviewed

Canopy effects on snow accumulation, observational study from lidar, canonical-view camera, and multi-year ground measurements

Zeshi Zheng ^{1*}, Qin Ma ², Kun Qian ³, and Roger Bales ^{1,2}

¹ Department of Civil and Environmental Engineering, University of California, Berkeley, CA, USA

² Sierra Nevada Research Institute, University of California, Merced, CA, USA

³ Department of Civil and Environmental Engineering, University of Texas, Austin, TX, USA

* Correspondence: zeshi.z@berkeley.edu

† Current address: Affiliation 3 †

‡ These authors contributed equally to this work. ‡

Academic Editor: name

Version July 15, 2018 submitted to Remote Sens.; Typeset by L^AT_EX using class file mdpi.cls

Abstract: A variety of canopy metrics were extracted from the snow-off airborne light detection and ranging (lidar) measurements over three study areas in the Sierra Nevada, Providence and Wolverton from the southern Sierra and Pinecrest in the central Sierra. More than 40 snow-depth sensors were deployed at Providence and Wolverton since 2008 and about 10 sensors were deployed at Pinecrest since 2014 for long-term snowpack measurements. At Wolverton, hemispherical-view images were captured and the sky-view factors were derived from the images at each individual zenith angle. We extracted the snow accumulation characteristics for each sensor measurements over multiple years. As the sensors were deployed under various canopy-cover conditions, we studied the variation of snow accumulation across landscape and found they are controlled by the canopy-cover conditions. We used regularized regression model Elastic Net to model the normalized snow accumulation with canopy metrics as independent variables, and found that about 50% of snow accumulation variability at each site can be explained by the canopy metrics from lidar.

1. Introduction

The snowpack in California's Sierra Nevada has long been served as the primary water resources for agricultural and urban uses [1]. For seasonal forecasts of flood peaks following the onset of snow melt, the estimation methods are turning from statistical estimates that use historical records to spatio-temporal

water-balance estimates with integrated data sources [2,3]. Quantifying the spatio-temporal distribution of snow accumulation allows more accurate forecast of snow melt and streamflow, but it is also a long-standing challenge in snow hydrology [4,5]. In the high Sierras, orographic effect drives solid-phase precipitations falling over mid-to-high elevation regions, where most areas are covered with heterogeneous densities and different types of vegetation [6,7]. During the snow accumulation period, the vegetation intercepts snowfall, causing snowpack distribute unevenly under canopy. As much as 60% of cumulative snowfall may be intercepted by forest in mid-winter and annual sublimation losses can be 30 – 40% of annual snowfall [8]. Being able to accurately quantify the canopy interception of snowfall is the foundation to estimate the total snow melt with higher accuracy and precision during the Spring season.

The canopy interception of snowfall can be quantified as the snow storage capacity of the canopy and interception efficiency (interception/snowfall). The snow storage capacity is the maximum amount of snowfall that can be intercepted by the canopy. It is determined by the leaf area, tree species, and initial canopy snow load [9]. The interception efficiency is found to decrease with increasing snowfall, initial canopy snow load and temperature. It increases with increasing leaf-area index and canopy coverage [8,10].

The coniferous canopies interception on snowfall is difficult to measure and quantify. Previous studies designed special weighing devices such that the weight of the intercepted snow accumulated snow can be measured at the same time. The total snow interception is found to be correlated with the accumulated snowfall [8,9]. Thus, several process models have incorporated this statistical finding and account canopy-cover effect on snow accumulation [11–14].

To calculate canopy interception, using canopy metrics that are highly correlated with the total snow accumulations is a common solution. Retrieving canopy metrics has advanced in recent years. The technology has been advancing from the traditional plant canopy analyzer [12,15–18], to hemispherical-view camera [19,20], and recently, to lidar [21,22]. The plant canopy analyzer was commonly used for retrieving the LAI in the forest. By using the hemispherical-view camera, the pixels of the taken images can be classified as either canopy-cover or clear, thus the percentage of clear view for each zenith angle can be quantified as sky-view factor, which was also found to be a statistically significant predictors for parameterizing snowfall interception in the process models [19,23]. The point-cloud data collected using lidar can be used for reconstructing the 3-dimensional canopy structures if the point-cloud has enough density. Algorithms have been developed for deriving LAI from

the lidar point clouds and it will be interested to develop new canopy metrics from lidar for quantifying the snowfall interception.

In addition to canopy-metric retrieval from lidar, the canopy effect can also be quantified by using statistical models, with dense spatial measurements of snow depth or snow water equivalent (SWE) [22, 23]. Most previous studies were conducted using lidar measurements, either airborne or terrestrial. Both the airborne and terrestrial lidar can provide dense spatial snow-depth measurements ($> 10\text{pts/m}$). With extensive footprint provided by airborne lidar scans, the canopy effect on snowpack spatial distribution can be quantified with large samples. The terrestrial lidar has a much smaller footprint comparing to airborne lidar [24], however, it is able to provide multiple scans per season. Thus the temporal variation in canopy effects can also be determined.

One short-coming in using lidar is it lacks temporal completeness, especially during the precipitation season, when it is difficult to take measurements. Lidar requires clear sky condition to take measurements to prevent the laser pulse intensity from attenuating because of rain drops and snow flakes [25]. A dense cluster of snow-depth sensors can compensate the weakness of lidar in terms of temporal consistency. Combining the vegetation structures derived from lidar measurements and continuous snow-depth measurements, there is potential that the spatial variation of snow accumulation can be accurately quantified. In our study, we used long-term spatially dense snow measurements in the Sierra Nevada, together with the lidar-derived canopy metrics, to study the canopy effect on seasonal snow accumulations.

The general objective of the work reported here is to explore the possibility of studying the spatial variability of snow accumulation by using lidar-derived canopy metrics and clustered snow-depth sensor measurements. We address two major question. First, to what extent can one use lidar-derived canopy metrics to predict the snow accumulation spatially. Second, for all developed lidar-derived canopy metrics, what is the relative importance between them.

2. Methods

2.1. Study areas and snow-depth sensor data

The study was conducted over three areas in the Sierra Nevada: Pinecrest in the Central Sierra, and Providence and Wolverton in the Southern Sierra (Figure 1(a)). For each study area, snow-depth sensors (Judd Communications) are instrumented and they are placed into clusters (Figure 1(b, c)), with topographic characteristics (elevation, aspect) varying between clusters and canopy-cover conditions

78 varying within each cluster. Pinecrest is the lowest in elevation and also flat in terms of elevation gradient.
 79 The lower site of Providence has similar elevation range as Pinecrest and the upper site is 200-m higher.
 80 Wolverton is the highest of the three study areas, with elevation around 2200 m at the lower site and 2600
 81 m at the upper site. The sensors in Pinecrest were installed in 2014 and the sensors in both Wolverton and
 82 Providence were installed back in 2008 (Table 1).

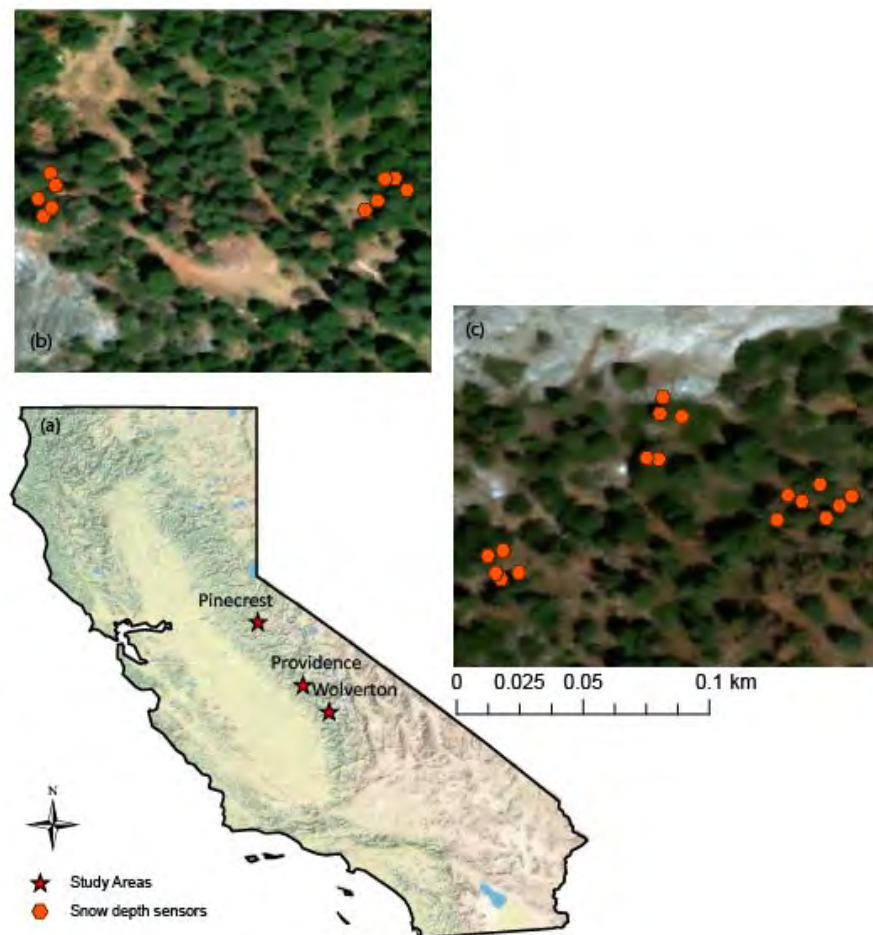


Figure 1. (a) The study areas locations in the Sierra Nevada. Snow-depth sensor locations around the (b) lower met stations and (c) upper met stations in the Providence site.

83 2.2. Lidar data

84 The point-cloud lidar data were used for generating raster data sets. The raw point-cloud files were
 85 divided into 250×250 -m tiles using LAStools lidar processing software. We extracted the ground points
 86 from each tile and interpolated them into a 0.5-m resolution digital elevation model (DEM) by using a
 87 simple kriging model with a spherical covariance function. The 250×250 -m DEM tiles were mosaicked

Table 1. Elevation information of each site and time-series data availability

Site	Sub-site	Elevation, m	Data availability
Pinecrest	Upper	1808 - 1834	WY2014-WY2017
	Lower	1748 - 1778	WY2014-WY2017
Providence	Upper	1975-1984	WY2008-WY2016
	Lower	1730-1740	WY2008-WY2016
Wolverton	Site1	2225-2227	WY2008-WY2016
	Site2	2250-2266	WY2008-WY2016
	Site3	2590-2602	WY2008-WY2016
	Site4	2630-2648	WY2008-WY2016

together to form a single DEM of the study area. Digital surface model (DSM) was generated from all first returns of the lidar point cloud. Subtracting the DEM from the DSM produces the canopy-height model (CHM). Individual tree was segmented out from the CHM using a watershed segmentation algorithm implemented in SAGA GIS software. Over each snow-depth sensor location, canopy metrics such as canopy height mean, standard deviation, and canopy density were extracted at searching radius from 2 m to 40 m with 1-m increment. Also, the distance from the sensor location to the closest tree trunk is also calculated.

2.3. Canonical-view images

The canonical-view images were taken below each individual sensor node, facing straight-up to the sky. The sky-view factors f at each individual zenith angle θ were derived from the raw image and the sky-view factor of the entire image is also estimated using the equation below,

$$f_{tot} = \frac{\int_{\theta=1}^{\theta=90} \sin(\theta) f(\theta)}{\int_{\theta=1}^{\theta=90} \sin(\theta)} \quad (1)$$

The sky-view factors data are available for Wolverton only. We included the total sky-view factor and the sky-view factors at each zenith angle as independent variables for modeling the snow accumulations observed at each sensor location. The results are compared with the modeled results that use lidar-derived canopy metrics as predictors, but over Wolverton only.

2.4. Snow accumulation events detection

The data availability over time for each site is shown in Table 1. To study the canopy effect on snow accumulation, we extracted all events when most precipitation is in solid form. This kind of events can be extracted from the time-series snow-depth data through the following procedure.

1. Get the moving average of each snow depth time-series with a window size of 2. Then calculate the 1st order gradient of time-series. This will make the following estimation invulnerable from high frequency noise in the snow depth data.
 2. The 1st order gradients over all sensors are used to calculate the $x\%$ quartile of the gradient. The quartile statistic was then compared with a pre-configured threshold to determine if most sensors observed snow accumulation. And the neighboring accumulating days were grouped together to form a single event.
 3. Quartile thresholds for snow precipitation and melting events are different. We set the quartile for snow accumulation as 30%. It means that if 30% of sensors show an ascending trend in one day, we can classify this day as an accumulation day.
 4. The daily gradient thresholds also need to be optimized, so do the gap length between two adjacent snow accumulation dates. The optimized threshold for snow accumulation events is 0.1 cm. And if two snow accumulation events were temporally close, we used the following rule to determine if the two neighboring events can be merged together or not.
- For snow accumulation events, the optimized way to combine two neighboring events together is to first judge if the length of gaps between two events are shorter than one third of the sum of length of two events. Then, if the snow depth data in most sensors doesn't show a descending trend during the gap period, the two closed events can be combined into one.

2.5. Statistical analysis

All extracted accumulation events are used for statistical modeling with features derived from the lidar data and the sky-view factors derived from the canonical-view camera images. We conducted regression analysis to study if canopy metrics can be used as predictors for estimating snow accumulating at various canopy-covered conditions. For each individual accumulation event, the total snow accumulation at each sensor node was estimated as $\Delta H = H_k - H_1$ where H_k is the snow-depth at the last time step and H_0 is the snow-depth at the initial time step. Considering the topographic effects on precipitation along the elevation gradient, we offset the total solid precipitation for each individual event at each site using topographic variables. The offset results are standardized to the range of 0 – 1. The detrended target values are regressed using Elastic Net, which is a regularized regression method that linearly combines both $L1$ and $L2$ penalties in the regression model. Assuming we have a linear regression problem defined as,

$$y = X\beta + \varepsilon \quad (2)$$

where y is the target value and X is the matrix of all covariates. The estimates of the regression coefficients $\hat{\beta}$ is defined as,

$$\hat{\beta} = \arg \min_{\beta} (\|y - X\beta\|^2 + \lambda_2 \|\beta\|^2 + \lambda_1 \|\beta\|_1) \quad (3)$$

The Elastic Net was chosen than other regularized regression approaches for its ability of addressing correlated covariates and when the number of covariates is high. In our case, the canopy metrics can be highly correlated when the searching radii are close and the number of covariates included in our analysis is more than 100.

In order to have representative estimate of how much variability that can be explained by the Elastic Net model. We used bootstrap to resample the data for 20 iterations and we estimated the cross-validated coefficient of determination (R^2) within each iteration. The distribution of the R^2 can be estimated from multiple bootstrapping results.

We also applied correlation analysis to explore the most informative radius of lidar-derived canopy features and the most informative zenith angle of the sky-view factors from the canonical view images. We correlated the snow accumulation from each individual event with the lidar-derived mean canopy height at various searching radii and at various zenith angles. The correlation coefficients R_s are compared at various radii and angles for selecting the optimal radius and zenith angle. Considering Pinecrest has a relatively short record, most of which is during the heavy drought of California, we did not conduct the analysis for Pinecrest. Also, camera images are not available for Providence thus we only radius dependency analysis at that site. For the data at Wolverton, we selected a few near-optimal searching radii and zenith angles. We used these selected variables and conducted a step-wise linear regression process for exploring the relative importance between variables.

3. Results

3.1. Snow accumulation events extracted from snow-depth time-series

We applied our snow accumulation events extraction algorithm on all snow-depth sensor clusters for all time periods when clean snow-depth data are available. The performance of the detection algorithm is similar to manual extraction that needs to be done by human. As is shown in Figure 2, the algorithm is

able to detect most major snow accumulation periods. And the summary of accumulation events detected for each site is shown in Table 2 and the distribution of the magnitude of the accumulation at each study area is shown in Figure 3.

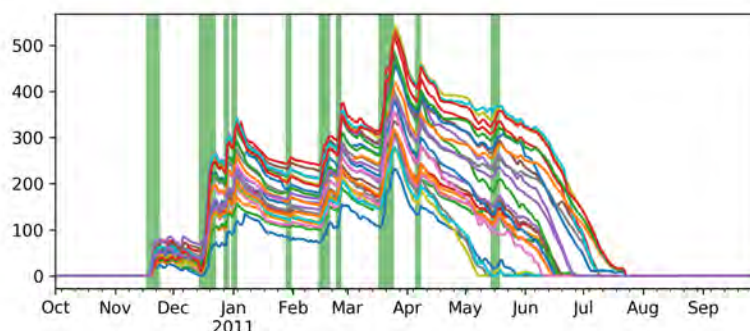


Figure 2. Snow accumulation events extracted using the accumulation detection algorithm, for Wolverton in 2011.

Table 2. Number of events detected for each water year from the three different study sites

Water Year	Providence	Wolverton	Pinecrest
2008	1	3	NaN
2009	6	8	NaN
2010	10	11	NaN
2011	7	10	NaN
2012	7	10	NaN
2013	7	5	NaN
2014	6	7	1
2015	5	8	3
2016	9	NaN	8
2017	NaN	NaN	8

3.2. Statistical modeling results

The variability that the Elastic Net model can explain over the three sites are shown as in Figure 4. The uncertainty range of the variability that can be explained by the Elastic Net model is much larger for the Pinecrest analysis than the other two areas. And the average of the explained variability decreases as the elevation becomes higher.

At Providence and Wolverton, excluding the minor accumulation events (≤ 15 cm) can significantly increase the variability that can be explained by the Elastic Net model, with more than 50% explained at Providence and 40%–50% explained at Wolverton. Due to the fact that for minor accumulation events the signal strengths are not significantly greater than the uncertainty range of the snow-depth sensors,

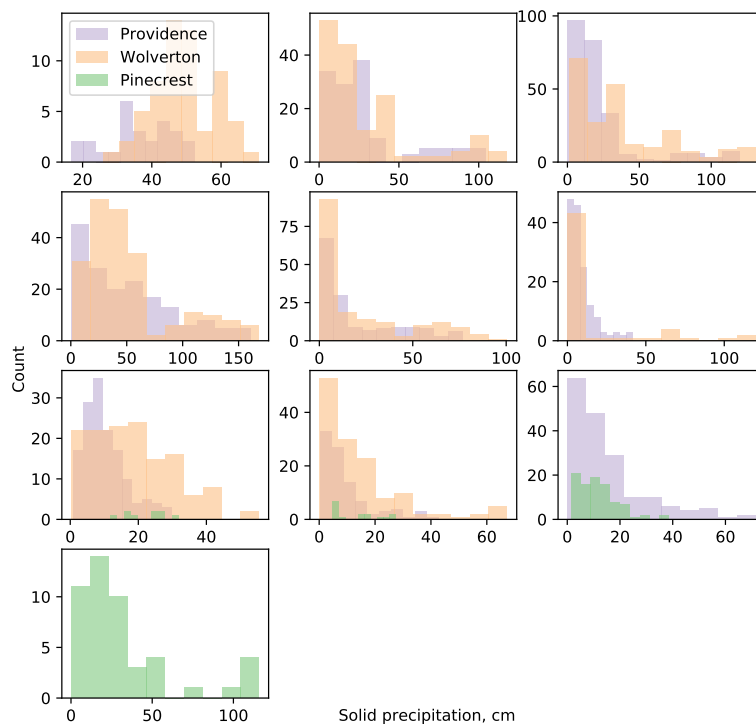


Figure 3. Solid-form precipitations distributions observed from three sites over 10 years

including these data points will defect the performance of the Elastic Net model. At Wolverton, the spatial variability of snow accumulation can be explained reaches the maximum when the mean snow accumulation is between 15 cm and 30 cm. At Pinecrest, no particular trends can be observed as the amount of data points is limited. When including most of the data points, the variability explained stabilized around 40%–60%.

Considering Wolverton is the only study area that both SVF and lidar are available and the trends observed in Figure 5. We constrained the valid mean precipitation in the range of 15–30 cm. We conducted three sets of analysis, including using lidar-derived canopy metrics as the predictors, using SVF as the predictors, and using both lidar and SVF as the predictors in the Elastic Net model. We did not observe much difference among the results from the three different sets of analysis. And the improvement of using both predictors is marginal (Figure 6).

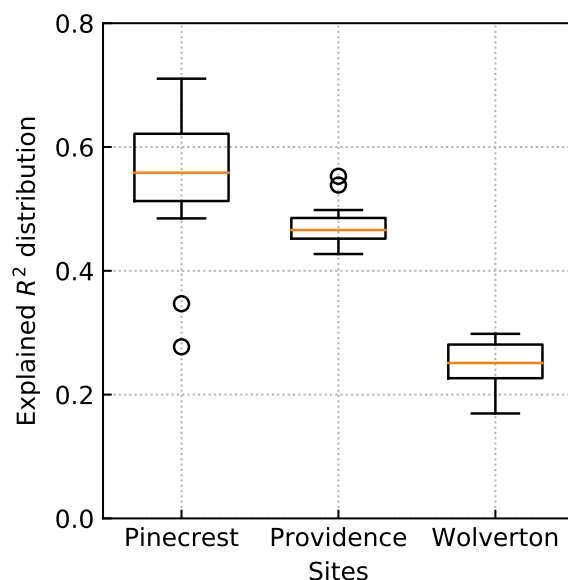


Figure 4. R^2 distribution over three sites

The correlation analysis (Figure 7(a)) show that the surrounding canopies have a stronger effect on the snow accumulation on the ground than the canopy right above. The canopy mean height within 15-m radius at Providence is the most effect distance while the optimal radius is about 8 m at Wolverton. For sky-view factor, the optimal zenith angle is about 21° at Wolverton. In Figure 7(a), we identify each individual precipitation event by the transparency of each curve, from which we can see that heavier storms have more dominant weights on characterizing the canopy effects at different searching radii from lidar data and zenith angles from canonical view imageries. In addition, the step-wise regression analysis conducted on the selected optimal variables of lidar-derived and canonical view imagery features suggest that the canonical view imagery features are more important and the marginal information that lidar provides is limited comparing to the first canonical view imagery feature selected.

In addition, we compared the correlation coefficient between different types of lidar-derived canopy-related features and the snow accumulation over different sensor nodes. The features include mean canopy height over the searching radius, standard deviation of the height, maximum canopy height, and canopy coverage. As is shown in Figure 8, the amount of data points at Pinecrest is not enough to draw solid conclusions. At Providence and Wolverton, the correlation coefficient, is a concave shaped function of both canopy-height mean and canopy coverage at various searching radii. The maximum canopy height at the smallest searching radius correlates the most with the snow

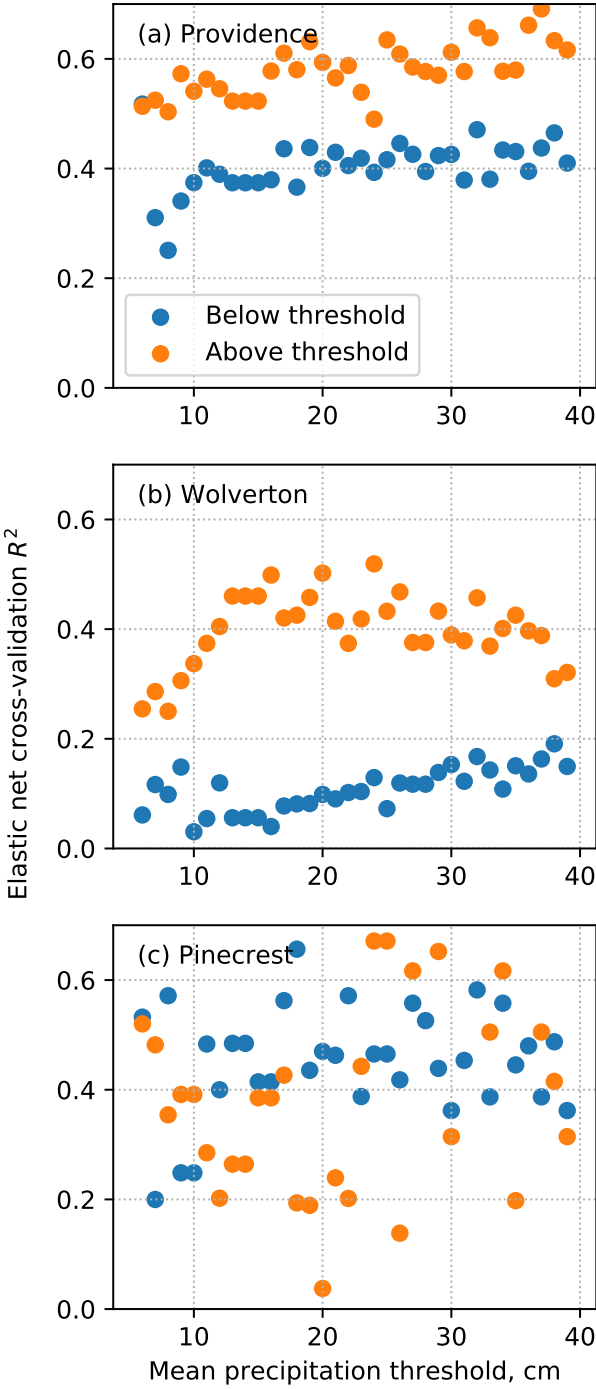


Figure 5. R^2 distribution over three sites vs. mean accumulation across sensors

202 accumulation. The standard deviations of the canopy heights at various searching radii show contrast
203 trends at Providence and Wolverton.

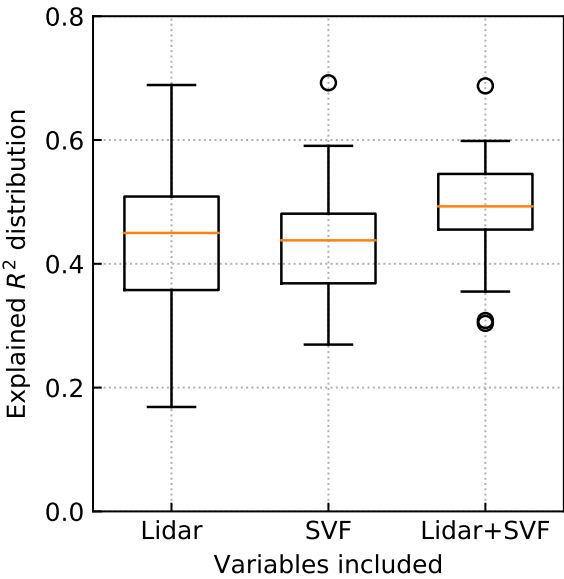


Figure 6. R^2 distribution over three sites vs. mean accumulation across sensors

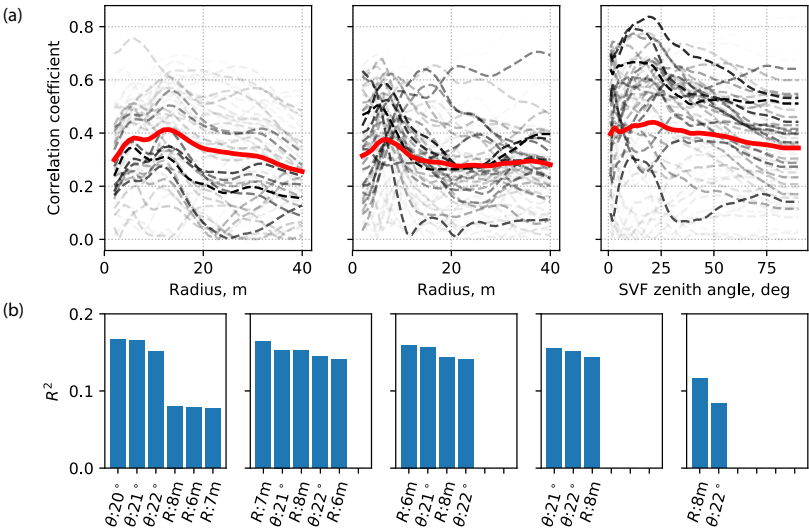


Figure 7. (a) Correlation coefficients estimated by correlating

4. Discussion

4.1. Canopy effect at different elevations

Among the three sites studied, the variability of snow accumulations that the canopy-related variables can explain vary from site to site and also depend on the mean cumulative precipitation over the entire event. The difference between sites can be attributable to different elevations as the

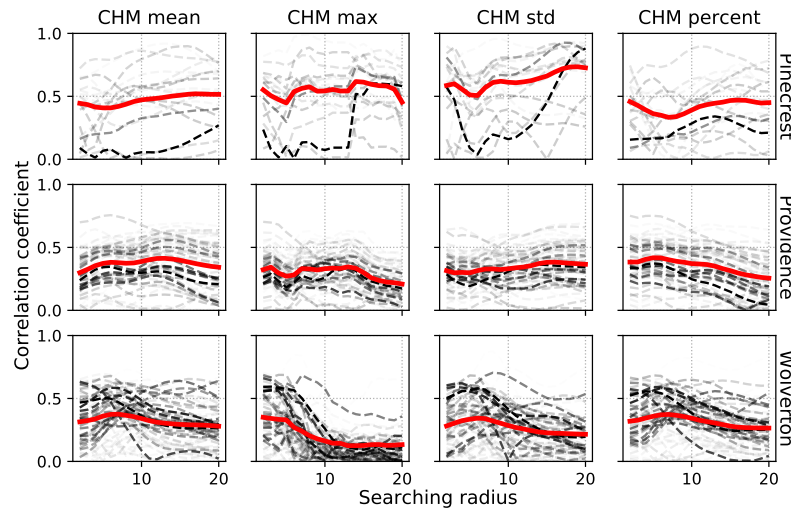


Figure 8. The correlation coefficient estimated between search radius and

canopy-cover density decreases as elevation increases and the solid phase precipitation increases with elevation. For example, the instrumentation locations at Pinecrest and Providence are at much lower elevations comparing to Wolverton. About 40% of snow-accumulation variability is attributable to the canopy effects at these two sites however only 25% can be explained over Wolverton. This suggests that at higher elevations, where precipitations are heavier, the canopy effects can be diluted by the heavy snowfall, which is similar to [10] has found, which stated that total interception of snowfall will saturate when the total precipitation reaches certain thresholds for different tree species. In addition, we observed some noise introduced by the low precipitation events in the regression analysis. Figure 5 suggests that the spatial variability of precipitation is less explainable by the canopy-related variables when the total precipitation is small.

4.2. Optimal variables characterizing canopy effects on snow accumulation

The canopy related variables derived from lidar and canonical-view images are compared. Based on Figure 6, the coefficient of determination calculated from 20 bootstrapping runs of predicting the snow accumulation suggests that the trained models are in lack stability in predicting the total snow accumulation at the unobserved sensor locations if using lidar-derived variables because the variability of the R^2 is larger than that using the sky-view factors. Also, the third box-plot of this figure suggests that the lidar-derived variables and sky-view factors are complementary and using both types variables can improve both R^2 and stability of prediction.

The snow-cover information is slightly more important than canopy metrics, including tree heights and tree-height standard deviations. This was verified by correlation coefficients in the regression analysis between snow accumulation and both tree height at increment searching radius and SVF at increment zenith angles. The SVFs are more correlated with snow accumulation than tree height in general. The step-wise regression analysis also suggested that sky-view factor at optimal zenith angle is more important than tree height at optimal searching radius. Although the tree height is an important metric characterizing trees in the forest but it does not necessarily represent the density and interception capacity of the canopy. Even sky-view factor only represents the canopy-cover condition at the lowest layer of canopy, it still explain partial variability in the interception capacity of the entire tree crown, which is the reason that it can be more important than lidar-derived canopy metrics.

Comparing within lidar-derived canopy metrics at increment radius, Figure 8 suggests that the most important canopy structures may not be the canopy layers right above the measured locations. The canopy surrounding within a few meters could be even more important as the interception capacity can be larger when the trees are clustered together than a single tree stand.

5. Conclusions

We found correlation between the lidar-derived canopy attribute and the snow accumulation extracted from the multi-year time-series snow-depth measurements. The correlation is stronger when the precipitation event has higher snow accumulation. And the correlation is also much stronger at a lower elevation because of denser vegetation. Although the lidar-derived canopy attributes are complementary to sky-view factor in explaining the snow-accumulation variability, the SVF is more important than lidar-derived variables when analyzing based on the step-wise regression. The canopy surrounding the snow surface within 8-m radius is more important than canopy structures within either smaller radius or larger radius, indicating clustered canopy effect is stronger than a single tree. The above findings suggest great potential of using lidar and ground measurements for studying canopy effect on mountain snowpack.

Acknowledgments: All sources of funding of the study should be disclosed. Please clearly indicate grants that you have received in support of your research work. Clearly state if you received funds for covering the costs to publish in open access.

Author Contributions: For research articles with several authors, a short paragraph specifying their individual contributions must be provided. The following statements should be used “X.X. and Y.Y. conceived and designed the experiments; X.X. performed the experiments; X.X. and Y.Y. analyzed the data; W.W. contributed

reagents/materials/analysis tools; Y.Y. wrote the paper.” Authorship must be limited to those who have contributed substantially to the work reported.

Conflicts of Interest: Declare conflicts of interest or state “The authors declare no conflict of interest.” Authors must identify and declare any personal circumstances or interest that may be perceived as inappropriately influencing the representation or interpretation of reported research results. Any role of the funding sponsors in the design of the study; in the collection, analyses or interpretation of data; in the writing of the manuscript, or in the decision to publish the results must be declared in this section. If there is no role, please state “The founding sponsors had no role in the design of the study; in the collection, analyses, or interpretation of data; in the writing of the manuscript, and in the decision to publish the results”.

Abbreviations

The following abbreviations are used in this manuscript:

MDPI: Multidisciplinary Digital Publishing Institute

DOAJ: Directory of open access journals

TLA: Three letter acronym

LD: linear dichroism

Bibliography

1. Bales, R.C.; Molotch, N.P.; Painter, T.H.; Dettinger, M.D.; Rice, R.; Dozier, J. Mountain hydrology of the western United States. *Water Resources Research* **2006**, *42*.
2. Zheng, Z.; Molotch, N.P.; Oroza, C.A.; Conklin, M.H.; Bales, R.C. Spatial snow water equivalent estimation for mountainous areas using wireless-sensor networks and remote-sensing products. *Remote Sensing of Environment* **2018**, *215*, 44–56.
3. Hopkinson, C.; Sitar, M.; Chasmer, L.; Gynan, C.; Agro, D.; Enter, R.; Foster, J.; Heels, N.; Hoffman, C.; Nillson, J.; Others. Mapping the spatial distribution of snowpack depth beneath a variable forest canopy using airborne laser altimetry. *Proceedings of the 58th Annual Eastern Snow Conference* **2001**.
4. Winstal, A.; Marks, D. Long-term snow distribution observations in a mountain catchment: Assessing variability, time stability, and the representativeness of an index site. *Water Resources Research* **2013**, *50*, 293–305.
5. Golding, D.L.; Swanson, R.H. Snow distribution patterns in clearings and adjacent forest. *Water Resources Research* **1986**, *22*, 1931–1940.
6. Houze, R.A. Orographic effects on precipitating clouds. *Reviews of Geophysics* **2012**, *50*.
7. Mott, R.; Scipión, D.; Schneebeli, M.; Dawes, N.; Berne, A.; Lehning, M. Orographic effects on snow deposition patterns in mountainous terrain. *Journal of Geophysical Research: Atmospheres* **2014**, *119*, 1419–1439.
8. Hedstrom, N.R.; Pomeroy, J.W. Measurements and modelling of snow interception in the boreal forest. *Hydrological Processes* **1998**, *12*, 1611–1625.
9. Pascal, S.; P., L.D.; M., B.S. Measurement of snow interception and canopy effects on snow accumulation and melt in a mountainous maritime climate, Oregon, United States. *Water Resources Research* **2002**, *38*, 5–1–5–16.
10. Schmidt, R.A.; Gluns, D.R. Snowfall interception on branches of three conifer species. *Canadian Journal of Forest Research* **1991**, *21*, 1262–1269.

11. Marks, D.; Domingo, J.; Susong, D.; Link, T.; Garen, D. A spatially distributed energy balance snowmelt model for application in mountain basins. *Hydrological Processes* **1999**, *13*, 1935–1959.
12. Hellström, R.A. Forest cover algorithms for estimating meteorological forcing in a numerical snow model. *Hydrological Processes* **2001**, *14*, 3239–3256.
13. Bartelt, P.; Lehning, M. A physical SNOWPACK model for the Swiss avalanche warning: Part I: numerical model. *Cold Regions Science and Technology* **2002**, *35*, 123 – 145.
14. Lehning, M.; Völksch, I.; Gustafsson, D.; Nguyen, T.A.; Stähli, M.; Zappa, M. ALPINE3D: a detailed model of mountain surface processes and its application to snow hydrology. *Hydrological Processes* **2006**, *20*, 2111–2128.
15. Gower, S.T.; Norman, J.M. Rapid Estimation of Leaf Area Index in Conifer and Broad-Leaf Plantations. *Ecology* **1991**, *72*, 1896–1900.
16. Stenberg, P.; Linder, S.; Smolander, H.; Flower-Ellis, J. Performance of the LAI-2000 plant canopy analyzer in estimating leaf area index of some Scots pine stands. *Tree Physiology* **1994**, *14*, 981–995.
17. Sturm, M.; Holmgren, J.; McFadden, J.P.; Liston, G.E.; III, F.S.C.; Racine, C.H. Snow–Shrub Interactions in Arctic Tundra: A Hypothesis with Climatic Implications. *Journal of Climate* **2001**, *14*, 336–344.
18. Pomeroy, J.W.; Gray, D.M.; Hedstrom, N.R.; Janowicz, J.R. Prediction of seasonal snow accumulation in cold climate forests. *Hydrological Processes* **2002**, *16*, 3543–3558.
19. Musselman, K.N.; Molotch, N.P.; Brooks, P.D. Effects of vegetation on snow accumulation and ablation in a mid-latitude sub-alpine forest. *Hydrological Processes* **2008**, *22*, 2767–2776.
20. Sirpa, R.; David, G.; Harri, K.; Ari, L.; Achim, G.; Olli-Kalle, K.; Ola, L.; Anders, L.; Kai, R.; Magnus, S.; Per, W. Estimation of winter leaf area index and sky view fraction for snow modelling in boreal coniferous forests: consequences on snow mass and energy balance. *Hydrological Processes* **2012**, *27*, 2876–2891.
21. Zheng, G.; Moskal, L.M. Retrieving Leaf Area Index (LAI) Using Remote Sensing: Theories, Methods and Sensors. *Sensors* **2009**, *9*, 2719–2745.
22. Zheng, Z.; Kirchner, P.B.; Bales, R.C. Topographic and vegetation effects on snow accumulation in the southern Sierra Nevada: a statistical summary from lidar data. *The Cryosphere* **2016**, *10*, 257–269.
23. Musselman, K.N.; Molotch, N.P.; Margulis, S.A.; Kirchner, P.B.; Bales, R.C. Influence of canopy structure and direct beam solar irradiance on snowmelt rates in a mixed conifer forest. *Agricultural and Forest Meteorology* **2012**, *161*, 46–56.
24. Revuelto, J.; López-Moreno, J.I.; Azorin-Molina, C.; Vicente-Serrano, S.M. Canopy influence on snow depth distribution in a pine stand determined from terrestrial laser data. *Water Resources Research* **2015**, *51*, 3476–3489.
25. Filgueira, A.; González-Jorge, H.; Lagüela, S.; Díaz-Vilariño, L.; Arias, P. Quantifying the influence of rain in LiDAR performance. *Measurement* **2017**, *95*, 143 – 148.

Sample Availability: Samples of the compounds are available from the authors.

© 2018 by the authors. Submitted to *Remote Sens.* for possible open access publication under the terms and conditions of the Creative Commons Attribution license (<http://creativecommons.org/licenses/by/4.0/>)